How the Anchoring Site on Two Extended Tetrathiafulvalenes Impacts the Electronic Communication through a Bis(acetylide)ruthenium Linker

Hadi Hachem, Antoine Vacher, Vincent Dorcet, Dominique Lorcy

HAL Id: hal-01559206

https://univ-rennes.hal.science/hal-01559206

Submitted on 13 Sep 2017

How the anchoring site on two extended tetrathiafulvalenes impacts the electronic communication through a bis(acetylide)ruthenium linker

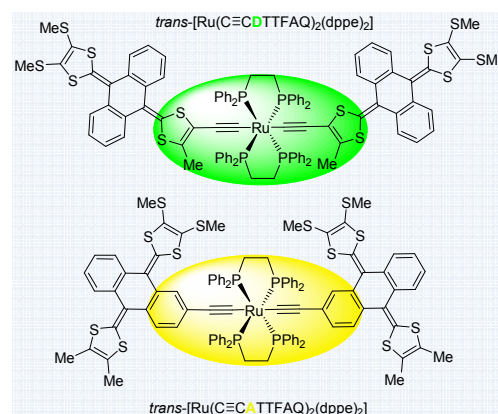Hadi Hachem, Antoine Vacher, Vincent Dorcet, Dominique Lorcy*

Institut des Sciences Chimiques de Rennes, UMR 6226 CNRS-Université de Rennes 1, Campus de Beaulieu, Bât 10A, 35042 Rennes cedex, France. Tel: 33 2 2323 6273; E-mail: Dominique.lorcy@univ-rennes1.fr,orcid.org/0000-0002-7698-8452

Abstract:

The interplay between two extended tetrathiafulvalenes connected, either from the dithiole rings or the anthraquinodimethane moieties, through a bis(acetylide) ruthenium linker has been studied within the novel complexes *trans*-[Ru(C≡C**D**TTFAQ)$_2$(dppe)$_2$] and *trans*-[Ru(C≡C**A**TTFAQ)$_2$(dppe)$_2$]. Cyclic voltammetry and spectro-electrochemical investigations evidence that the organic and inorganic electrophores are electronically coupled within these complexes. Moreover, the electronic communication between the two organic electrophores depends on the localization of the anchoring site of the organometallic bis(acetylide) ruthenium linker on the organic electrophores.

Introduction

Extended tetrathiafulvalenes, where two 1,3-dithiole rings are connected in 2-position by an anthraquinodimethane core (TTFAQs), have focused a lot of the attention as building blocks for the design of molecular materials for artificial photosynthesis and photovoltaics,[1,2] molecular receptors,[3] molecular tweezers for C_{60}[4] or metal ions.[5] The TTFAQ is a redox active moiety which exhibits pronounced structural changes associated with electron transfer.[6,7] Indeed, in the neutral state, due to steric hindrance, the molecule adopts a saddle/butterfly shape, while in the dicationic state, the generated anthracene central part becomes planar with the two dithiole moieties localized in perpendicular planes.[8] This molecular motion concerted with the electron transfer leads to pseudo reversible cyclic voltammogram where the compound oxidizes into the dication with potential inversion.[9,10] TTFAQ dimers have also been synthetized either as macrocyclic receptors for C_{60} recognition[11,12] or as positive electrode materials for rechargeable batteries.[13] In order to form TTFAQ dimers, different strategies have been used: either the two redox active cores are directly connected to each other, or a spacer group is used. Moreover, the link between the two TTFAQ moieties can be localized either between two dithiole rings or between two anthraquinodimethane cores. Two different redox behaviors are observed: dimers where both TTFAQ are oxidized simultaneously and dimers where each electroactive core is oxidized sequentially. This second case is scarce.[13,14] On the one hand, when the two donor moieties are covalently attached by the anthracene cores with a spacer (A in chart 1), such as an oxygen atom,[15] an ethene[16], alkyne[17,18] or more recently a Pt bis(acetylide) linker,[12] both TTFAQ are oxidized simultaneously and no electronic interplay has been evidenced. On the other hand , when the TTFAQs are linked directly through the dithiole moieties (B and C chart 1), two closely spaced redox processes are observed, indicating intramolecular electronic interactions between the donor units.[14]

Chart 1

X = O, CH=CH, CC
 cis-Ptbis(acetylide)

R$_1$=R$_2$=H
R$_1$=R$_2$=SMe
R$_1$=H;R$_2$=SMe

A

B

C
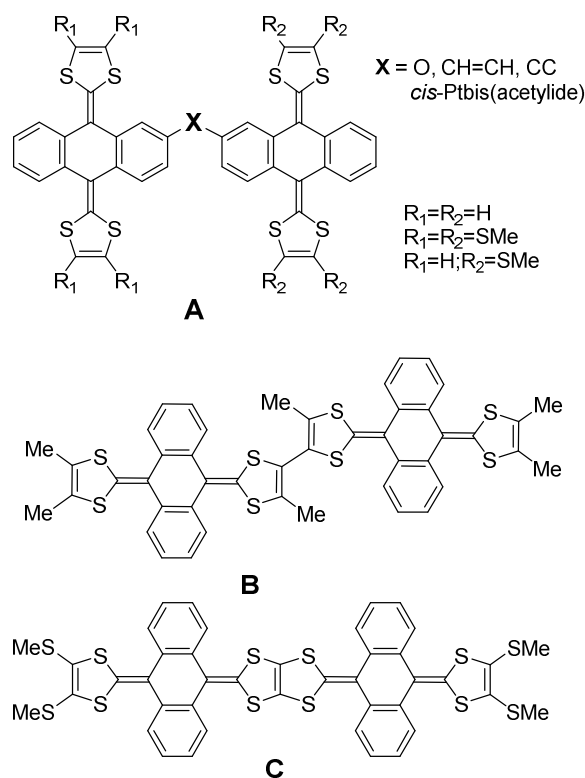
Recently, we reported the synthesis of TTF dimers where the two redox active cores are connected by an organometallic linker the *trans*-Ru-bis(acetylide) and we demonstrated that electronic communication occurs between the three redox active cores, i.e. the two TTF and the Ru centre within *trans*-[Ru(C≡CMe$_3$TTF)$_2$(dppe)$_2$].[19] The bis(acetylide)ruthenium linker is indeed known to promote the electronic interactions in both the Fc[20] and TTF[19] series. Thus, we decided to investigate similar TTFAQ dimers, *trans*-[Ru(C≡CTTFAQ)$_2$(dppe)$_2$] (Chart 2). In order to analyze the effect of the anchoring site of the organometallic fragment on the electronic interplay, we prepared two types of complex, either the one where the bis(acetylide)ruthenium linker is covalently attached to the dithiole ring of each donor, *trans*-[Ru(C≡C**D**TTFAQ)$_2$(dppe)$_2$] noted as D-Ru-D, or to the anthraquinodimethane core of the donor, *trans*-[Ru(C≡C**A**TTFAQ)$_2$(dppe)$_2$] noted as A-Ru-A (Chart 2).

Chart 2

trans-[Ru(C≡C**D**TTFAQ)₂(dppe)₂]

*trans*-[Ru(C≡C**A**TTFAQ)₂(dppe)₂]

trans-[RuCl(C≡C**D**TTFAQ)(dppe)₂]
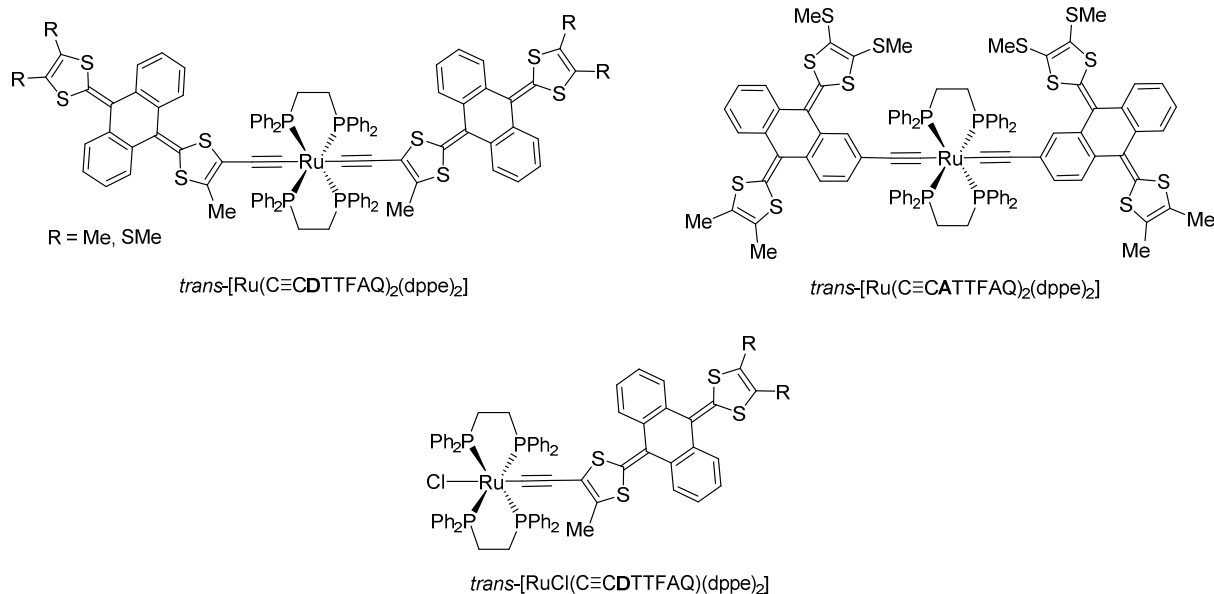
Herein, we report the synthesis of the two types of TTFAQ dimers and their electrochemical and spectroelectrochemical investigations, in order to characterize the electronic interactions between the TTFAQ units. In addition, to gain a better insight into the possible interaction between Ru and the TTFAQ, we also synthetized and characterized the mono substituted complex, where only one donor core is connected to the Ru atom *via* an alkyne bridge, *trans*-[RuCl(C≡C**D**TTFAQ)(dppe)₂] noted as D-Ru (chart 2).

Results and Discussion

The target alkyne derivatives **3a-b** were prepared starting from the iodo-TTFAQ **1a-b** according to the chemical route described in Scheme 1. Sonogashira type reaction between **1a**[14]**-b** and trimethylsilylacetylene catalyzed by CuI and PdCl₂(PPh₃)₂ in the presence of diisopropylamine afforded **2a-b** in good yields. Deprotection of the alkyne, perfomed by adding KF into a solution of **2a-b** in MeOH, afforded TTFAQ **3a-b** in quantitative yields.
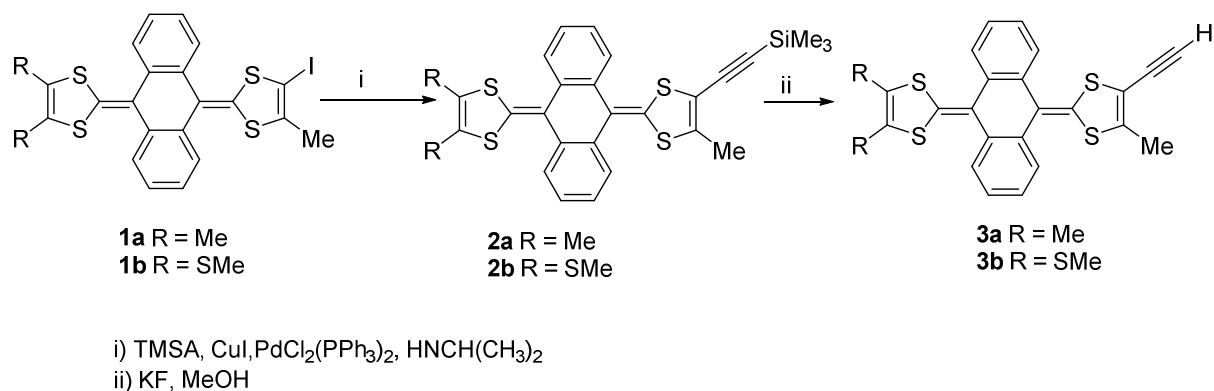
Scheme 1. Synthesis of the TTFAQ-ethyne **3a-b**.

Crystals of **3a** suitable for X-ray diffraction study were grown by slow concentration of chloroform solution. TTFAQ **3a** crystallizes with one molecule of $CHCl_3$ and the molecular structure of **3a** is represented in Figure 1. The TTFAQ exhibits a saddle like shape with bond lengths and bond angles of the TTFAQ core itself in the usual range for such derivatives.[8,21] The C≡C distance in **3a** (1.151(7) Å) is comparable with that of Me_3TTF-ethyne (1.152(8) Å).[19]
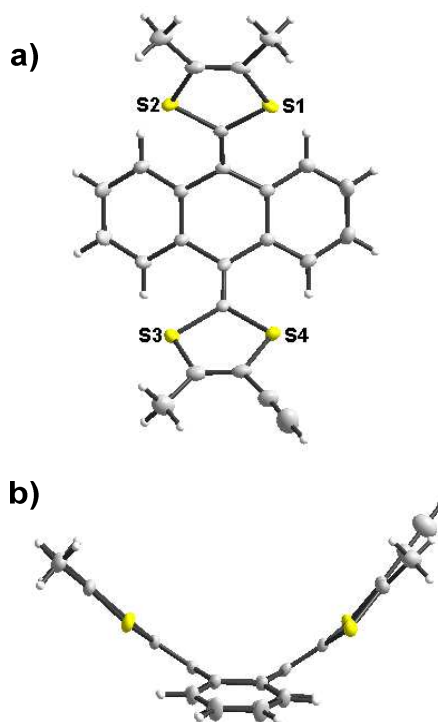

Figure 1. Molecular structure of **3a** (a) showing thermal ellipsoids at 50 % probability level (b) side view.
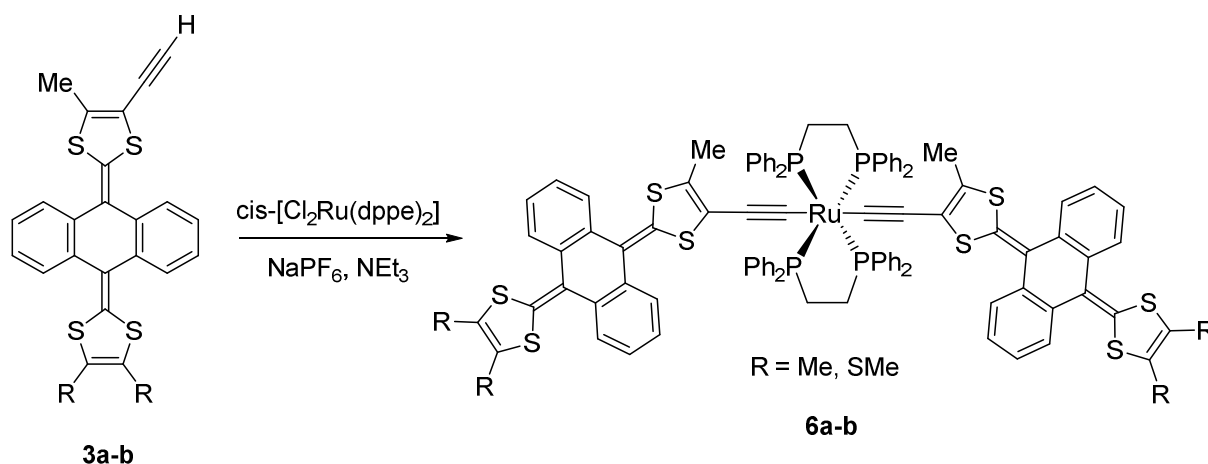
The synthesis of *trans*-[RuCl(C≡C**D**TTFAQ)(dppe)$_2$] **5a-b**, D-Ru, is based on the reaction of TTFAQ-ethyne **3a-b** with [ClRu(dppe)$_2$][OTf] in dichloromethane at room temperature under inert atmosphere (scheme 2). The progress of the reaction was monitored by ^{31}P NMR: the two triplets of [ClRu(dppe)$_2$][OTf] at 84.9 and 57.1 ppm gradually disappear, and a new singlet appears at δ 46.5 and 46.6 ppm for **4a** and **4b** respectively. This singlet is assigned to a vinylidene intermediate **4a-b** that could be isolated as a greenish powder. To reach the desired complex, deprotonation of the vinylidene was achieved *via* the addition of triethylamine under inert atmosphere. After the addition of base, an immediate change of color from green to yellow was observed, and the complexes *trans*-[RuCl(C≡C**D**TTFAQ)(dppe)$_2$] **5a-b** were obtained as yellowish solid (scheme 2). ^{31}P NMR showed the presence of two close multiplets at δ 50.7 and 50.1 ppm for **5a** (Figure S1) and δ 49.7 and 48.6 ppm for **5b**. This result might be explained by the adoption of a favored position in space for the TTFAQ molecule which results in the slight break of symmetry between the phosphorus atoms.
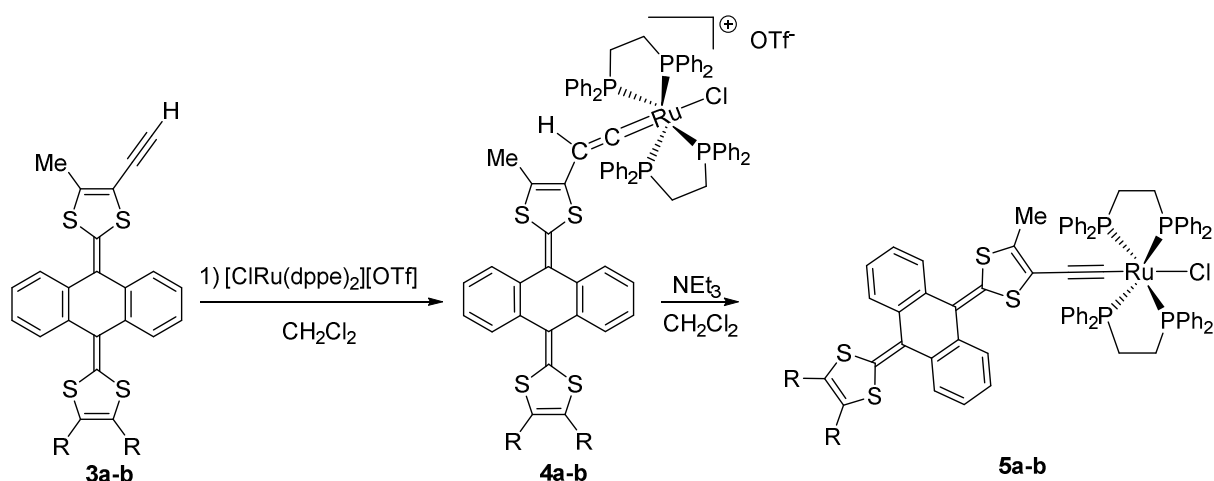
Scheme 2. Synthesis of *trans*-[RuCl(C≡C**D**TTFAQ)(dppe)$_2$] **5a-b** (**a**: R = Me, **b**: R = SMe).

The dimeric TTFAQ complexes D-Ru-D **6a-b** were synthesized by the reaction of TTFAQ alkyne **3a-b** with *cis*-Cl$_2$Ru(dppe)$_2$ in the presence of NaPF$_6$ and NEt$_3$ under inert atmosphere

at room temperature in dichloromethane (Scheme 3). Complex **6a** was obtained as a yellow powder, insoluble in common organic solvents, while the presence of the SMe groups on the TTFAQ cores slightly increases the solubility of **6b**. ^{31}P NMR spectrum of the later complex shows one singlet at δ 51.8 ppm indicating equivalent phosphorus surrounding and a *trans* arrangement of the acetylide ligands around the metallic center.

Scheme 3. Synthesis of *trans*-[Ru(C≡C**D**TTFAQ)₂(dppe)₂] **6a-b** (**a**: R = Me, **b**: R = SMe).

In order to analyze the effect of the localization of the connection on the donor core on the electronic properties of the complex, we also prepared the reference complex A-Ru-A **8** where the two TTFAQs are linked by the organometallic bridge connected to the anthracene core. This was carried out using similar conditions as the one described above for **6a-b** but using TTFAQ-ethyne **7** with *cis*-Cl₂Ru(dppe)₂ in the presence of NaPF₆ and NEt₃ (Scheme 4). ^{31}P NMR spectrum of this complex shows one singlet at δ 53.9 ppm, confirming a *trans* arrangement as observed for the previous complex D-Ru-D **6b**. Nevertheless, this signal is observed at lower field than for D-Ru-D **6b** due to the localization of the anchoring site on the anthraquinone moiety which exerts a less electron releasing effect than the dithiole ring. Complex **8** was obtained in 45 % yield as an orange powder.
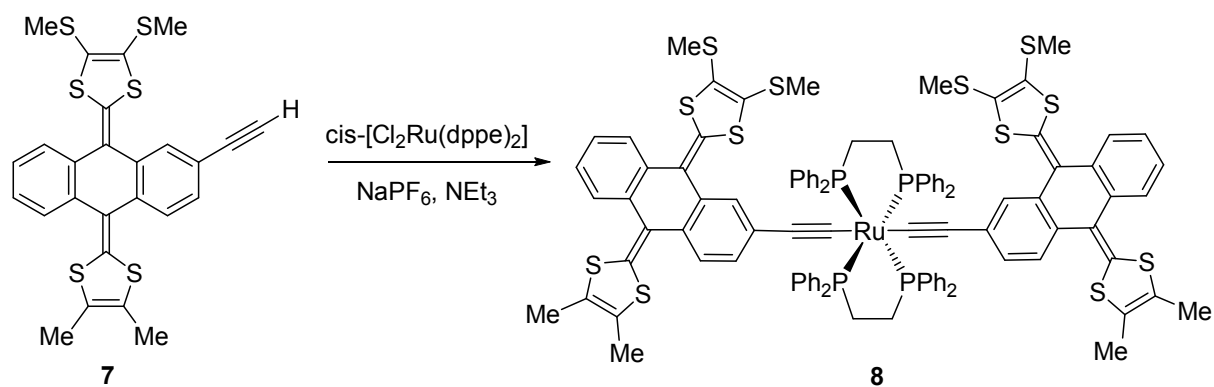
Scheme 4. Synthesis of *trans*-[Ru(C≡CATTFAQ)$_2$(dppe)$_2$] **8**.

IR spectroscopy.

The stretching frequency of the alkyne bond measured with IR spectroscopy gives preliminary insights on the degree of conjugation between the redox active moities. TTFAQ-ethyne **3a-b** exhibit IR stretching vibration bands localized at $\nu_{C≡C}$ = 2095-2096 cm^{-1} respectively. In complexes D-Ru **5a** and D-Ru-D **6a-b**, the $\nu_{C≡C}$ stretching frequency is found at 2044 cm^{-1}, close to the one found for the *trans*-[Ru(C≡CMe$_3$TTF)$_2$(dppe)$_2$][19] and *trans*-[RuCl(C≡CMe$_3$TTF)(dppe)$_2$][22] complexes (2033 and 2029 cm^{-1} respectively). This indicates a high degree of conjugation in all these Ru complexes, D-Ru **5a-b** and D-Ru-D **6a-b**. The IR spectrum of A-Ru-A **8** reveals a stretching vibration band at 2053 cm^{-1}, characteristic of aromatics linked to the ruthenium atom *via* an acetylide bridge.[23] The $\nu_{C≡C}$ stretching frequencies of complexes D-Ru-D **6a-b** where the connection occurs through the dithiole ring, is lower by 10 cm^{-1}, due to a higher electron donor character of the dithiole ring than the anthraquinodimethane moiety. Similar influences were already observed on the ^{31}P NMR spectra of these complexes (see above).

Single crystals of complex D-Ru-D **6b** were obtained by slow diffusion of pentane into a concentrated solution of **6b** in chloroform and carbon disulfide (3/1) under an inert atmosphere. The molecular structure of **6b**, presented in Figure 2, shows that two TTFAQ-acetylide ligands are coordinated to the ruthenium center in a *trans* arrangement. The Ru-bis(acetylide) spacer is almost linear with angles at Cα–Ru–Cα, Ru–Cα≡Cβ and

Cα≡Cβ–CTTF of 180.00°, 174.33° and 175.27° respectively. The Ru–C distance of 2.065(4) Å and the C≡C bond length of 1.212 (5) Å for **6b** are similar to those observed for *trans*-[Ru(C≡CMe₃TTF)₂(dppe)₂] (2.069(3) Å and 1.203(3) Å respectively).[19] As already noticed for other Ru bis(acetylide) complexes, the alkyne bond in the D-Ru-D complex **6b** is much longer than in TTAFQ **3a** (1.151(7) Å). As observed in Figure 2 both TTFAQ cores exhibit the classical saddle like shape.
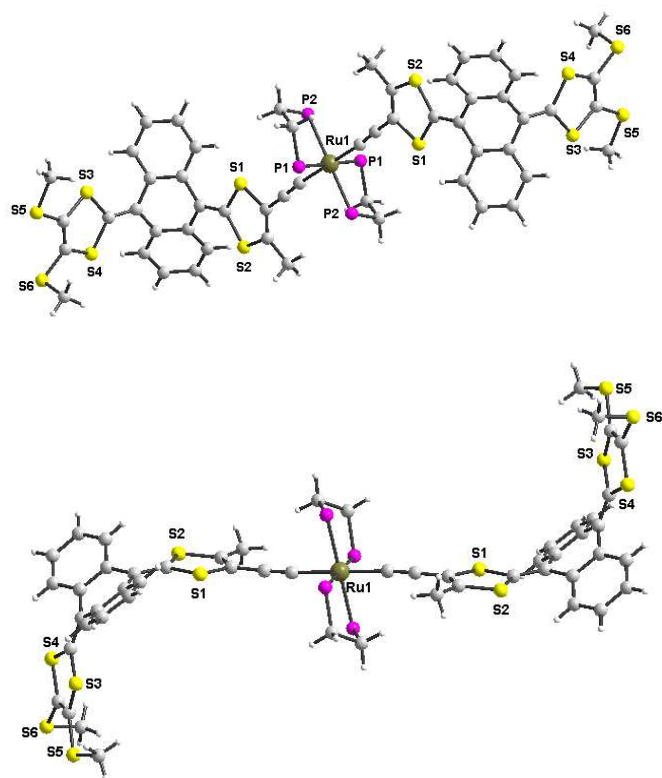
Figure 2. Two views of the molecular structure of *trans*-[Ru(C≡C**D**TTFAQ)₂(dppe)₂] **6b**. The phenyl substituants of the two dppe ligands have been omitted for clarity.

Electrochemical properties

The redox properties of the TTFAQ derivatives **1a-b**, **3a-b**, **7** and the complexes D-Ru **5a-b**, D-Ru-D **6b** and A-Ru-A **8** were studied by cyclic voltammetry (CV), performed in CH₂Cl₂ containing 0.1 M of Bu₄NPF₆ as supporting electrolyte. The redox potentials are given in V *vs*

Fc/Fc$^+$ and are collected in Table 1. The CVs of the starting TTFAQs **1-3** and **7** exhibit a single two-electron, quasi-reversible oxidation wave corresponding to the oxidation of the TTFAQ from the neutral state to the dication (Figure 3) which is the typical behavior observed for such TTFAQ donors.[24,25] The differences between the anodic and the cathodic peak potentials ($\Delta E_p = E_{Pa} - E_{Pc}$) amount to 290-210 mV for the different TTFAQs studied at 100mV/s. The large separation between the anodic and cathodic peaks is generated by the major conformational change that accompanies the electron-transfer process. It is a typical example of inverted potentials in a two-electron process, where it is easier to remove the second electron than the first one.[9] The redox potentials do not vary significantly for compounds **1** to **3** indicating the similar influence of the iodo substituent (**1**) and the alkyne one (**2-3**). Between the two series, **a** and **b**, the thiomethyl substituents decrease slightly the overall donating ability, as the redox potentials are shift towards anodic potentials by 20 to 50 mV. For **7**, with the ethyne arm on the anthraquinodimethane moiety, substituted by two Me groups and two SMe groups, the redox properties are closed to the one observed for **3a**.

Table 1 Redox potentials in CH_2Cl_2, Epa/Epc in V vs Fc/Fc$^+$, ΔEp in mV

compound	R = Me **a**	R = SMe **b**
I-TTFAQ **1**	0.03/-0.26 (290)	0.05/-0.16 (210)
Me$_3$SiC≡C-TTFAQ **2**	0.02/-0.27(290)	0.06/-0.17 (230)
H-C≡C-TTFAQ **3**	0.03/-0.24 (270)	0.08/-0.16 (240)
H-C≡C-TTFAQ **7**	0.02/-0.22 (240)	
D-Ru **5a**	-0.20/-0.50 (300), 0.52/0.45 (70)	
D-Ru **5a**	-0.12/-0.37 (250), 0.53/0.46 (70)	
D-Ru-D **6b**	-0.14/-0.26 (120), -0.08/-0.18 (100), 0.70/0.65 (50)	
A-Ru-A **8**	-0.11/-0.16 (50), 0.22/0.29 (70)	

For complex D-Ru **5a-b**, with one single TTFAQ moiety, two redox systems are observed on the CVs, one pseudo reversible bielectronic system (ΔE_p = 300 and 250 mV for **5a-b**) and a fully reversible monoelectronic process (ΔE_p 70 mV), (Figure 3). Both processes are tentatively assigned respectively to the redox signature of the TTFAQ core and the Ru organometallic fragment. The pseudo reversible system is observed at a lower potential than the one observed for the starting TTFAQ **3**, with a potential shift of 200-230 mV. The second process at 0.49 V is thus viewed as involving essentially the Ru^{II}/Ru^{III} couple. This process is anodically shifted by 430 mV compared to the one observed for *trans*-[RuCl$_2$(dppe)$_2$] analyzed in the same conditions (0.06 V). This indicates that the oxidation of the metal center is strongly affected by the presence of the TTFAQ dication in its close proximity. These observations are reminiscent to those realized in the TTF series where the two electrophores, the TTF and the Ru, were strongly electronically coupled.[19]
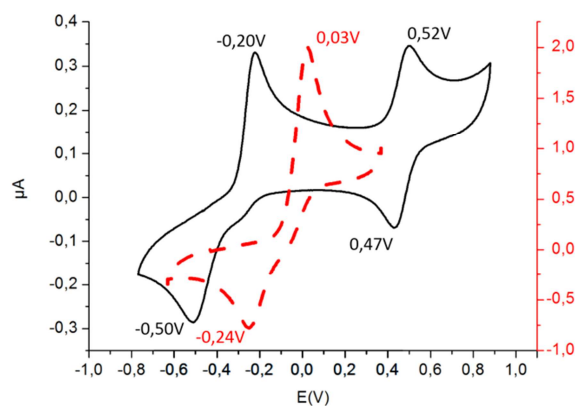
Figure 3. Cyclic voltammograms in CH_2Cl_2 with 0.1 M of Bu_4NPF_6 at 0.1 V s^{-1} of complex **5a** (black solid line) and **3a** (red dashed line), V vs Fc/Fc$^+$.

Due to solubility problems, we did not investigated the redox behavior of D-Ru-D **6a**, but we analyzed the thiomethyl substituted D-Ru-D **6b** and the CV is presented in Figure 4 together with the CV of the non metallated TTFAQ-ethyne **3b** in the same experimental conditions for comparison. For D-Ru-D **6b**, three clear oxidation peaks are observed indicating the stepwise

formation of four redox states from the neutral state to the pentacation. The two first oxidation peaks are assigned to the sequential oxidation of the two TTAFQ cores to TTFAQ dications with a potential difference of 60 mV, and finally the third oxidation peaks at 0.67 V is attributed to the Ru^{II}/Ru^{III} couple.
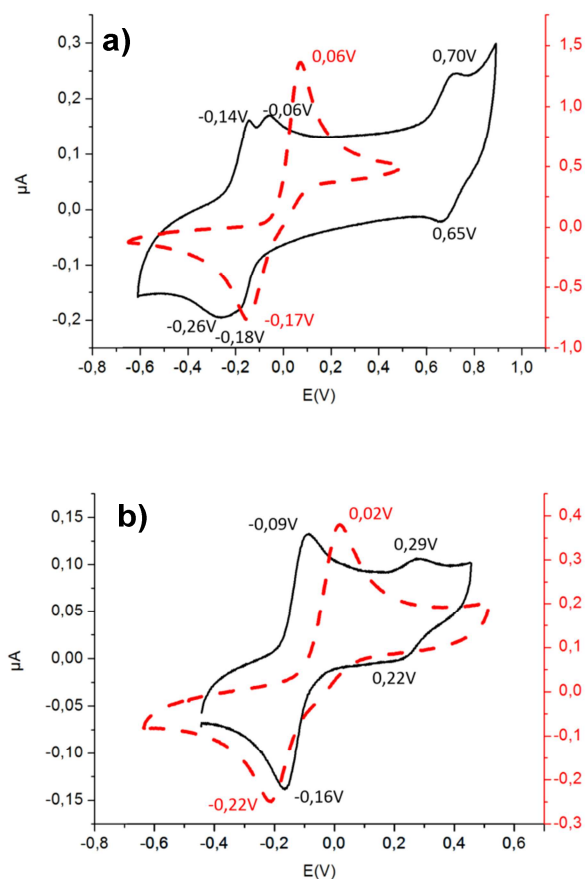
Figure 4. Cyclic voltammograms in CH_2Cl_2 with 0.1 M of Bu_4NPF_6 at 0.1 V s^{-1}, V vs Fc/Fc^+, of a) complex D-Ru-D **6b** (black solid line) and **3b** (red dashed line), b) complex A-Ru-A **8** (black solid line) and the starting TTFAQ ethyne **7** (red dashed line).

As previously observed for D-Ru **5a-b**, the oxidation of the two TTFAQ moieties within D-Ru-D **6b** occurs at a lower potential (by 200 mV) than the starting TTFAQ alkyne **3b** (Figure 4a). This can be ascribed to an increase of the electron density on the TTFAQ moiety thanks to the presence of the electron rich organometallic fragment. The existence of two close

oxidation waves for the two TTFAQ moieties suggests a sizeable electronic interaction between the two moieties through the ruthenium bis(acetylide) linker. The last oxidation process is then assigned to the oxidation of the ruthenium, which is anodically shifted by 610 mV compared with the redox potentials observed for *trans*-[RuCl$_2$(dppe)$_2$]. This larger shift is due to the existence of two TTFAQ, each under the dicationic state, in the close proximity of the Ru atom, which are acting as strong electron acceptors. Their effect is efficiently transmitted to the metal center *via* the acetylide linkers.

For complex A-Ru-A **8**, where the site of connection to the ruthenium is located on the anthraquinodimethane ring, a fully different CV than those obtained for complexes D-Ru **5a-b** and D-Ru-D **6b** is observed (Figure 4b). Two reversible oxidation waves at E^1 = -0.13 V and E^2 = 0.25 V are attributed to the simultaneous oxidation of the two TTFAQ cores into the TTFAQ^{2+}, with the exchange of 4 e$^-$, followed by the oxidation of the Ru center. This result was confirmed by a DPV study where the two peaks appeared with a ratio of 4:1 (Figure S2). Thus, the connection through the central anthraquinodimethane ring of the TTFAQ does not allow, at the CV scale, the observation of interplay between the two TTFAQ cores, but it leads to a highly reversible redox process in contrast to the precursor **7**. Another interesting feature is the influence of the organometallic part on the redox potentials of the TTFAQ cores. Indeed the oxidation peak potential of the TTFAQ cores within complex A-Ru-A **8** is only cathodically shifted by 100 mV while for the previous complexes D-Ru **5** and D-Ru-D **6b** the shift was more pronounced (200 mV). The smaller cathodic shift observed for the redox process assigned to the TTFAQ cores indicates that the electron donating effect of the Ru is less efficiently transmitted through the anthraquinodimethane moiety. This can be easily explained by the fact that in TTFAQ, the HOMO is mainly located on the dithiole rings and the LUMO on the anthraquinodimethane unit.[14] In the same vein, the oxidation potential of the Ru^{II}/Ru^{III} couple is only anodically shifted by 190 mV compared with the one observed

for *trans*-[RuCl$_2$(dppe)$_2$] (0.06 V) while for complex D-Ru-D **6b** an anodic shift of 610 mV was observed. The generation of the TTFAQ^{2+} induces the aromatization of the dithiolium rings together with that of the central anthracene which lies in a plane perpendicular to the planes of the dithiolium rings. Therefore the dithiolium rings act now as acceptor whose effect is weakly transmitted *via* the anthracene acetylide to the Ru center.

Spectroelectrochemical UV-vis-NIR investigations UV-vis-NIR spectra of the neutral starting alkyne **3a-b** and **7** carried out on dichloromethane solution (c ≈ 5.10^{-5} M) are reported in Figure 5. The TTFAQ **3a-b** exhibit two absorption bands in the UV-vis range at λ_{max} = 436 nm (ε = 27000 Lmol^{-1}cm^{-1}) and 368 nm (16000 Lmol^{-1}cm^{-1}) for **3a**, typical for TTFAQ derivatives and only a small hypsochromic shift of 4 nm is observed for **3b** on each absorption bands (432 and 364 nm).[16] Concerning TTFAQ **7**, the presence of the ethyne fragment on the anthraquinodimethane moiety leads to a red shift of the energy transitions of 14 and 10 nm respectively for the two absorption bands at 450 nm (ε = 26000 Lmol^{-1}cm^{-1}) and 378 nm (ε = 15500 Lmol^{-1}cm^{-1}). Upon oxidation to the dicationic state, the two absorption bands observed in the neutral state gradually decrease in intensity, whereas a broad absorption band centered at 500 nm increases with an isosbestic point at 460 nm. This absorption band is characteristic of the TTFAQ^{2+} absorption.[26] Very similar evolution of the spectra was already observed upon oxidation of a TTFAQ derivative.[14]
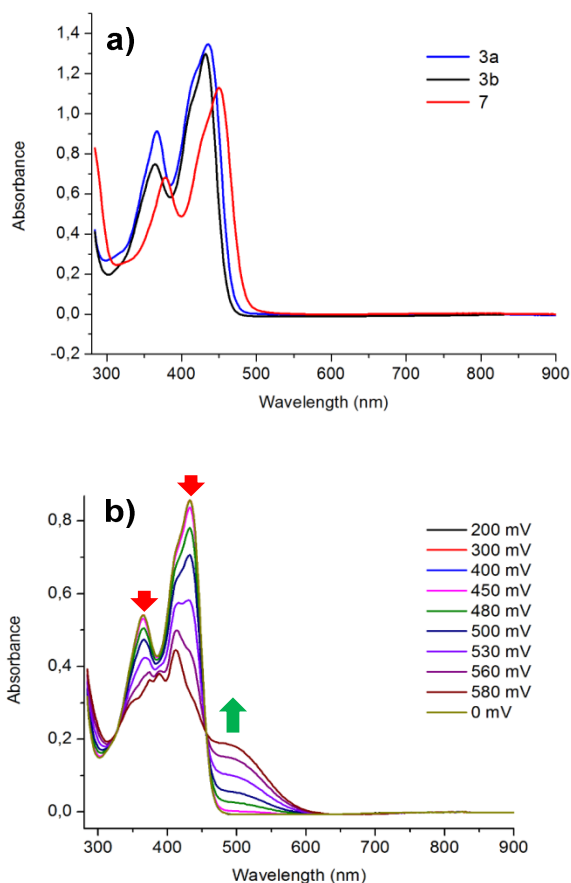
Figure 5 a) UV-vis-NIR spectra of TTFAQ-ethyne **3a**, **3b**, and **7**, b) UV-vis-NIR monitoring of the electrochemical oxidation of **3b** in CH_2Cl_2 containing 0.2 M Bu_4NPF_6 , potentials are quoted *vs* SCE.

Spectroelectrochemical UV-vis-NIR investigations were also carried out on metal complexes D-Ru **5a**, D-Ru-D **6b** and A-Ru-A **8** in the same experimental conditions. The neutral complex D-Ru **5a**, involving one single TTFAQ, exhibits three absorption bands in the UV-vis region at 464 nm ($\varepsilon = 16640$ $Lmol^{-1}cm^{-1}$), 394 nm ($\varepsilon = 12360$ $Lmol^{-1}cm^{-1}$) and 330 nm ($\varepsilon = 13300$ $Lmol^{-1}cm^{-1}$) . The latter is ascribed to a metal-to-ligand charge transfer transition (MLCT) while the lowest energy absorption is assigned to a $\pi-\pi^*$ transition which is red shifted by 28 nm compared to the TTFAQ alkyne **3a** (436 nm). Upon gradual oxidation to **5a**$^{2+}$, D^{2+}-Ru, a decrease of the absorption bands at 464 and 330 nm and the increase of the band at 394 nm bands occur together with the appearance of a broad absorption band at 660

nm (Figure 6). A clear isosbestic point emerges at 510 nm. The evolution of the UV-vis-NIR spectra of D-Ru **5a** upon gradual oxidation strongly differs from the spectra obtained for **3a** since for **3a**[2+] there is no absorption beyond 600 nm. The broad band observed for D-Ru **5a**[2+], TTFAQ[2+]-Ru, at 660 nm is reminiscent to what was observed with the TTF complex *trans*-[RuCl(C≡CMe$_3$TTF)(dppe)$_2$][22] where such a broad band was observed at an even lower energy (1399 nm) and was then ascribed to a SOMO-LUMO transition. Herein, it suggests that electronic interactions take place between the TTFAQ[2+] and the Ru center along the acetylide linker. The TTFAQ dication acts as a good acceptor and the Ru center as an electron donor, thus the band observed at 660 nm for **5a**[2+] can be viewed as an intramolecular charge transfer (ICT) band.[27] In accordance, upon oxidation to the tricationic state **5a**[3+], TTFAQ[2+]-Ru[III], this band disappears (Figure S3). The spectrum of **5a** is fully recovered upon reduction of **5a**[3+]. It is worth mentioning that compared with all the spectroelectrochemical investigations reported on TTFAQs up to now, none of them exhibit upon oxidation to the dicationic state such a broad absorption band at low energy.

Figure 6. UV-vis-NIR monitoring of the electrochemical oxidation of **5a** in CH$_2$Cl$_2$ containing 0.2 M Bu$_4$NPF$_6$, potentials are quoted *vs* SCE.

Let us consider now the metal complexes involving two TTFAQ linked through the Ru bis(acetylide) linker anchored on the dithiole ring, D-Ru-D **6b**, or on the anthraquinodimethane moiety, A-Ru-A **8**, of the organic electrophores. The UV-vis absorption spectrum of complex **6b** shows two absorption band at low energies at 468 and 372 nm which are red shifted by 36 nm for the lowest energy one compared to the TTFAQ-ethyne **3b** (Figure 7a). This shift is more important than the one observed for the monosubstituted complex D-Ru **5a**.

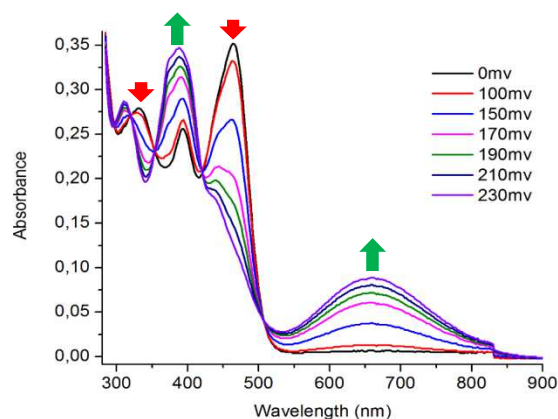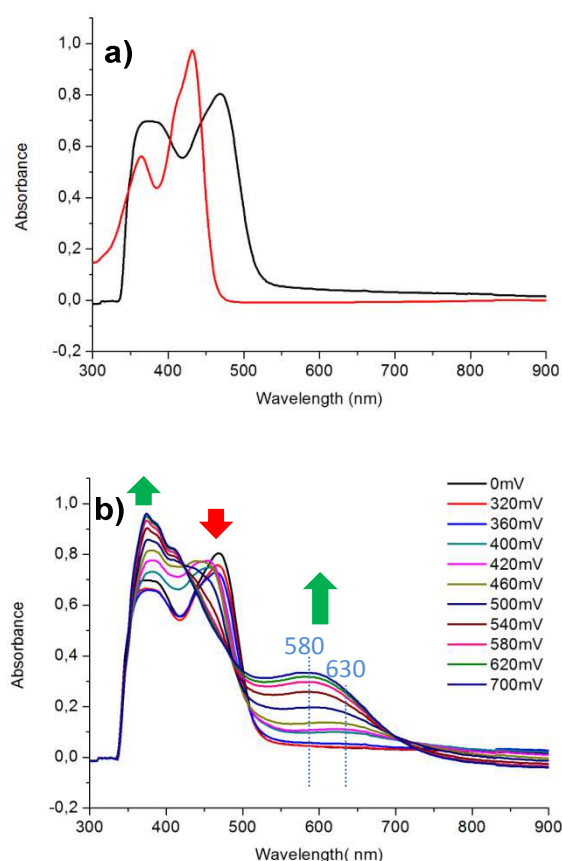**Figure 7.** a) UV-vis-NIR spectra of D-Ru-D **6b** (black line) and **3b** (red line), b) UV-vis-NIR monitoring of the electrochemical oxidation of **6b** in CH_2Cl_2 containing 0.2 M Bu_4NPF_6, potentials are quoted *vs* SCE.

Upon gradual oxidation of the bis-acetylide complex D-Ru-D **6b** to the first oxidation potential corresponding to the oxidation of one TTFAQ moiety a broad band centered at 630

nm appears (Figure 7b, Figure S4). This is reminiscent to what was observed for the mono acetylide complex D-Ru **5a** and can be attributed to an Intramolecular Charge Transfer (ICT) from the Ru towards the TTFAQ^{2+} which behaves as an acceptor. Oxidation to the tetracation induces a further increase of this absorption band together with a shift towards higher energy as the maximum wavelengths reaches 580 nm. This ICT band at 580 nm collapses upon oxidation of the metallic center (Figure S5). The spectrum of the neutral specie is recovered after sequential reduction of the pentacation.

The UV-vis-NIR spectrum of complex A-Ru-A **8** is similar to that of TTFAQ-ethyne **7** with two absorption bands at 450 nm and 382 nm (Figure 8a). Spectroelectrochemical investigations carried out on complex A-Ru-A **8** results in the decrease of the absorption band at 450 nm and the appearance of a broad band at 580 nm. If we compare now the two complexes D-Ru-D **6b** and A-Ru-A **8**, a different evolution of the spectra upon oxidation to the tetracation is observed. For the complex D-Ru-D **6b**, upon oxidation to the dication **6b**$^{2+}$ the intensity of the lowest energy band gradually increases and a shift of 50 nm towards higher energies was detected while oxidizing the dication **6b**$^{2+}$ to the tetracation **6b**$^{4+}$. Whereas the oxidation of complex A-Ru-A **8** to the tetracation **8**$^{4+}$ the oxidation leads only to the growth of the band centered at 580 nm. The behavior observed for **6b** is similar to that observed for the TTF complex, *trans*-[Ru(C≡CMe$_3$TTF)$_2$(dppe)$_2$],[19] and consistent with the existence of electronic interplay between the two TTFAQ in **6b** across the organometallic linker.
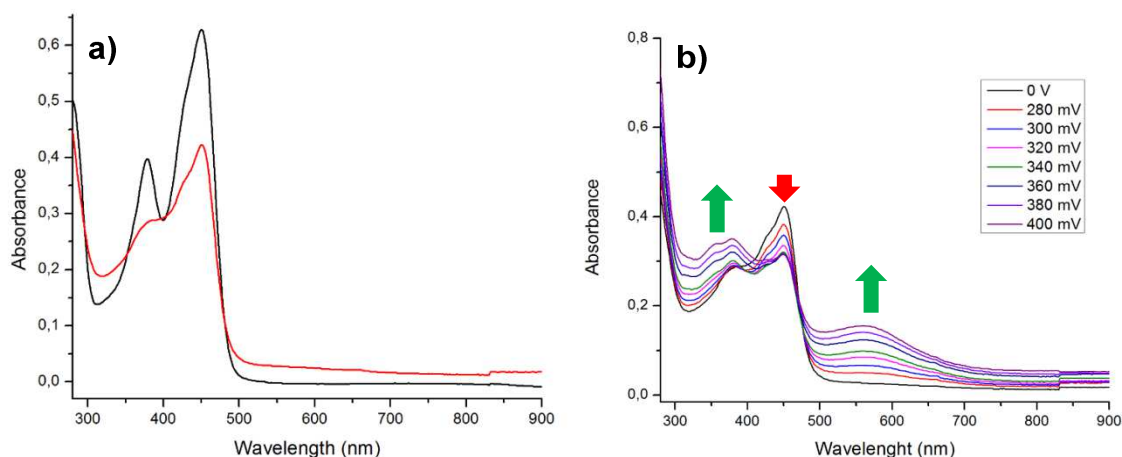
Figure 8. a) UV-vis-NIR spectra of A-Ru-A **8** in red and **7** in black, b) UV-vis-NIR monitoring of the electrochemical oxidation of **8** in CH_2Cl_2 containing 0.2 M Bu_4NPF_6, potentials are quoted *vs* SCE.

Conclusion

In summary, we have reported here the synthesis of three types of electroactive ruthenium complexes bearing either one or two extended tetrathiafulvalene, TTFAQ, connected to a Ru center by an acetylide linker. The influence of the anchoring site of the linker on the TTFAQ core on the electronic coupling between the different electrophores has been investigated by a combination of electrochemical and spectroelectrochemical investigations. In all three complexes (D-Ru, D-Ru-D and A-Ru-A) electronic interactions between the TTFAQ and the Ru have been evidenced. However intramolecular interactions between two TTFAQs are only observed when a Ru bis(acetylide) linker is localized on the dithiole rings of the TTFAQ moieties (D-Ru-D). These results demonstrate how important is the localization of the linker between two TTFAQ units for allowing intramolecular electronic coupling between these two electrophores.

Experimental section

General. NMR spectra were recorded at room temperature using CDCl$_3$ unless otherwise noted. Chemical shifts are reported in ppm and ^{1}H NMR spectra were referenced to residual CHCl$_3$ (7.26 ppm), ^{13}C NMR spectra were referenced to CHCl$_3$ (77.2 ppm) and ^{31}P NMR to H$_3$PO$_4$. Mass spectra were recorded with Agilent 6510 instrument for organics compounds, and with Thermo-fisher Q-Exactive instrument for complexes by the Centre Régional de Mesures Physiques de l'Ouest, Rennes. CVs were carried out on a 10^{-3} M solution of complex in CH$_2$Cl$_2$-[NBu$_4$][PF$_6$] 0.1 M. CVs were recorded on a Biologic SP-50 Instruments at 0.1 Vs^{-1} on a platinum disk electrode. Potentials were measured *versus* KCl Saturated Calomel Electrode (SCE), calibrated using internal ferrocene. The spectroelectrochemical setup was performed in CH$_2$Cl$_2$-[NBu$_4$][PF$_6$] 0.2 M using a Pt grid as the working electrode, a Pt wire as the counter electrode and SCE reference electrode. A Shimatzu 3600 spectrophotometer was employed to record the UV-vis-NIR spectra. Column chromatography was performed using silica gel Merck 60 (70-260 mesh). All other reagents and materials from commercial sources were used without further purification. The complexes were synthetized under an argon atmosphere using standard Schlenk techniques. The solvents were purified and dried by standard methods. The *cis*-[RuCl$_2$(dppe)$_2$][28] and TTFAQ **1a**[14] and **7**[29] were synthesized according to literature procedure. The synthesis of **1b** is described in supporting information.

Trimethylsilylethynyl-TTFAQ 2(a-b). In a Schlenk tube, the iodo-TTFAQ (550 mg for **1a** and 650 mg for **1b**, 1 mmol) together with PdCl$_2$(PPh$_3$)$_2$ (74 mg, 0.1 mmol) and CuI (20 mg, 0.1 mmol) were placed under vacuum for 5 hours. Then the solids were solubilized in 40 mL of dry THF and 0.5 mL of diisopropylamine and trimethylsilylacetylene (0.25 mL, 1.75 mmol) were quickly added. The reaction mixture was stirred at room temperature for 48

hours. The solvent was evaporated and the resulting solid was purified by flash chromatography on silica gel using dichloromethane/petroleum ether (2:8) as eluent. TTFAQ **2a-b** were obtained as yellow solid in 70 and 80% yield respectively.

2a mp > 220°C: ^{1}HNMR δ 7.64 (m, 2H), 7.56 (m, 2H), 7.26 (m, 4H), 2.10 (s, 3H), 1.93 (s, 6H), 0.20 (s, 9H). ^{13}C NMR 136.7, 126.0, 125.6, 125.3, 120.8, 108.2, 101.6, 94.6, 15.2, 13.1, 0.2; HRMR calcd for $C_{28}H_{26}S_4Si$: 518.0681. Found : 518.0677; Anal. calcd. for $C_{28}H_{26}S_4Si$: C, 64.82; H, 5.05; S, 24.72%. Found C, 64.52; H, 5.11; S, 24.25%.

2b mp > 220°C; ^{1}HNMR: δ 7.6 (m, 2H), 7.54 (m, 2H), 7.29 (m, 4H), 2.39 (s, 6H, 2(SMe)), 2.12 (s, 3H, Me), 0.20 (s, 9H, Si(Me)$_3$); ^{13}C NMR 136.7, 134.8, 134.7, 134.6, 134.5, 132.1, 130.9, 126.2, 126.2, 126.1, 125.9, 125.6, 125.4, 125.4, 125.4, 123.8, 122.9, 108.3, 101.9, 94.4, 19.2, 15.2; HRMR calcd for $C_{28}H_{26}S_6Si$: 582.0123. Found : 582.0127; Anal. calcd. for $C_{28}H_{26}S_6Si$: C, 57.69; H, 4.50%. Found C, 58.05; H, 4.25%.

TTFAQ-ethyne 3a-b To a solution of **2** (1 mmol, 520 mg for **2a** and 580 mg for **2b**) in 100 mL of methanol KF (100 mg, 1.7 mmol) was added. The reaction mixture was stirred for 15 h under argon at room temperature. The solvent was removed in vacuo and the residue was purified by column chromatography on silica gel using dichloromethan/petroleum ether (1/9) as eluent. TTFAQ-ethyne 3a-b were obtained as yellow powder in 98 and 94 % yield respectively.

3a mp > 220°C; ^{1}H NMR: δ 7.65 (m, 2H), 7.56 (m, 2H), 7.27 (m, 4H), 3.29 (s, 1H), 2.12 (s, 3H), 1.93 (s, 6H); ^{13}C NMR δ 137.64, 135.27, 134.72, 133.86, 131.05, 126.12, 125.72, 125.64, 125.42, 125.33, 125.24, 123.48, 120.89, 106.99, 83.54, 74.36, 15.12, 13.09; IR (KBr): $\upsilon_{C\equiv C}$ = 2095 cm^{-1}; HRMS calcd for $C_{25}H_{18}S_4$: 446.0286. Found : 446.0281; Anal. calcd. for $C_{25}H_{18}S_4$: C, 67.23; H, 4.06; S, 28.71%. Found C, 66.57; H, 4.18; S, 28.69%.

3b mp > 220°C; ^{1}HNMR: δ 7.57 (m, 4H), 7.3 (m, 4H), 3.31(s, 1H; ≡CH), 2.39 (s, 6H, 2(SMe)), 2.13 (s, 3H; Me); ^{13}CNMR: δ 137.6, 134.7, 134.7, 134.6, 134.6, 131.8, 131.1, 126.3, 126.2, 125.9, 125.6, 125.5, 125.4, 125.3, 123.7, 123.0, 107.1, 83.7, 74.1, 19.2, 15.1; IR (KBr): $υ_{C≡C}$ = 2096 cm^{-1}; HRMS calcd for $C_{25}H_{18}S_6$: 509.9727. Found : 509.9727; Anal. calcd. for $C_{25}H_{18}S_6$: C, 58.78; H, 3.55; S, 37.66%. Found C, 58.42; H, 3.17; S, 38.13%

Complexes **5a-b:** A solution of TTFAQ **3** (0.6 mmol, 270 mg for **3a** and 310 mg for **3b**) in 15 mL of CH_2Cl_2 was added to a solution of [ClRu(dppe)$_2$][OTf] (480 mg, 0.48 mmol) in 15 mL of CH_2Cl_2. After 24 h of stirring at room temperature, the solvent was removed in vacuo and the precipitate was washed with diethyl ether. The dark green precipitate, the vinylidene derivative [**4**][TfO] was used in the next step without further purification. ^{31}P NMR (121 MHz, CDCl$_3$) δ 46.5 (s, 4P) for **4a** and 46.5 (s, 4P) for **4b**. The vinylidene derivative [**4**][TfO] was dissolved in 30 mL of CH_2Cl_2 and NEt$_3$ (1 mL) was added an immediate change of color from green to yellow was observed. The reaction mixture was stirred at room temperature for 2 h and the solvent was removed under vacuo. The resulting powder was washed with distilled water (3x 20 mL) and pentane (3x 20 mL). Complex **5a** was obtained as a yellow powder in 40 % yield. ^{1}H NMR: δ 7.80 (m, 8H), 7.67 (m, 4H), 7.30-7.24 (m, 9H), 7.13 (m, 12H), 6.91 (m, 15H), 2.78 (m, 4H), 2.54 (m, 4H), 1.95 (s, 6H), 1.28 (s, 3H); ^{31}P NMR: δ 50.7 (m, 2P), 50.1 (m, 2P); ^{13}C NMR δ 136.5, 135.7, 135.4, 135.3, 134.9, 134.8, 133.9, 132.1, 129.5, 128.4, 127.5, 126.7, 125.7, 125.6, 125.5, 125.3, 125.2, 125.1, 121.8, 120.8, 120.8, 120.1, 114.0, 104.8, 34.1, 30.8, 22.3, 14.0, 13.5, 13.1. IR (KBr): $υ_{C≡C}$ = 2044 cm^{-1}; HRMS calcd for $C_{77}H_{65}ClP_4RuS_4$: 1378.1646; Found : 1378.1654.

5b ^{1}H NMR (CD$_2$Cl$_2$) δ 7.75-7.00 (m, 48H); 2.84 (m, 4H); 2.66 (m, 4H); 2.45 (s, 3H); 2.43 (s, 3H); 1.32 (s, 3H); ^{31}P NMR (CD$_2$Cl$_2$) δ 49.7 (m, 2P); 48.6 (m, 2P); ^{13}C NMR (CD$_2$Cl$_2$) δ

136.7, 136.4, 136.3, 135.8, 135.2, 135.2, 134.9, 134.8, 134.7, 134.6, 134.5, 134.23, 134.2, 134.1, 134.0, 133.9, 129.8, 129.4, 128.7, 128.6, 127.5, 127.4, 126.83, 126.8, 126.2, 125.8, 125.7, 125.4, 125.3, 124.5, 119.5, 114.0, 104.1, 30.7, 18.9, 13.4; IR (KBr): $\upsilon_{C\equiv C}$ = 2044 cm^{-1} ; HRMS calcd for $C_{77}H_{65}ClP_4RuS_6$: 1442.1087; Found : 1442.1102.

Complexes **6a-b** and **8**: To a solution of TTFAQ-ethyne (0.87 mmol, 390 mg for **3a**, 440 mg for **3b** and 460 mg for **7**), cis-[RuCl$_2$(dppe)$_2$] (0.35 mmol, 338 mg) and NaPF6 (1.74 mmol, 300 mg) in CH$_2$Cl$_2$ (40 mL), freshly distilled NEt$_3$ (1 mL) was added and the solution was stirred at room temperature for 15 hours. The reaction mixture was filtered and the precipitate was washed with distilled water (4 x 40 mL) and dry Et$_2$O (3 x 40 mL). Complexes **6a-b** and **8** were isolated as yellow powders in 55% yield, 60 % and 45% yields respectively. Complex **6a** was insoluble in common organic solvent. Complex **6b** was crystallized by slow diffusion of pentane into a solution of **6b** in CHCl$_3$ and carbon disulfide (3/1).

6a IR (KBr): $\upsilon_{C\equiv C}$ = 2044 cm^{-1}; HRMS calcd for $C_{102}H_{82}P_4RuS_8$: 1788.2170; Found :1788.2168; Anal. calcd. for [$C_{102}H_{82}P_4RuS_4 +_{0.5}CH_2Cl_2$]: C, 67.21; H, 4.57. Found C, 67.34; H, 4.45.

6b ^{1}HNMR (CD$_2$Cl$_2$) δ 7.64 (m, 5H), 7.49 (m, 5H), 7.31(m, 21H), 7.15 (m, 9H), 7.00 (m, 6H), 2.62 (m, 8H, (dppe)$_2$), 2.43 (s, 6H, 2(SMe)), 2.39 (s, 6H, 2(SMe)), 1.24(s, 6H, 2(Me)); ^{31}P NMR (CD$_2$Cl$_2$) δ 51.8 (s, 4P); ^{13}C NMR (CD$_2$Cl$_2$): δ (ppm) 136.0, 135.7, 135.3, 134.5, 134.1, 134.0, 129.7, 129.0, 127.3, 126.1, 126.0, 125.7, 125.6, 125.5, 125.3, 121.4, 119.5, 114.4, 106.3, 31.5, 19.2, 14.1; IR (KBr): $\upsilon_{C\equiv C}$ = 2044 cm^{-1}; HRMS calcd for $C_{102}H_{82}P_4RuS_{12}$: 1916.1053. Found : 1916.1062; Anal. calcd. for $C_{102}H_{82}P_4RuS_{12}$: C, 63.89; H, 4.31; S, 20.06%. Found C, 63.74; H, 4.38; S, 19.51%.

8 ^{31}P NMR δ 53.9 (s, 4P); IR (KBr): $\upsilon_{C\equiv C}$ = 2053 cm^{-1}; HRMS calcd for $C_{104}H_{86}P_4RuS_{12}$: 1944.13667. Found : 1944.1366. Anal. calcd. for [$C_{104}H_{86}P_4RuS_{12} + CH_2Cl_2$]: C, 62.11; H, 4.37; S, 18.95%. Found C, 62.57; H, 4.36; S, 19.24%.

Crystallography. Single-crystal diffraction data were collected on a D8 VENTURE Bruker AXS diffractometer (Mo- Kα radiation, λ = 0.71073 Å). The structure were solved by dual-space algorithm using the SHELXT program,[30] and then refined with full-matrix least-square methods based on F2 (SHELXL-2014).[31] All non-hydrogen atoms were refined with anisotropic atomic displacement parameters. H atoms were finally included in their calculated positions. Details of the final refinements are given in Table 2.

Table 2 Crystallographic data for TTFAQ **3a** and *trans*-[Ru(C≡C**D**TTFAQ)$_2$(dppe)$_2$] **6b**.

Compound	3a	6b
Formulae	C$_{25}$H$_{18}$S$_4$, CHCl$_3$	C$_{102}$H$_{82}$P$_4$RuS$_{12}$, 3(CHCl$_3$)
FW (g.mol^{-1})	566.00	2275.45
System	triclinic	triclinic
Space group	P-1	P-1
a (Å)	8.9594(10)	10.7345(8)
b (Å)	9.6392(11)	13.9086(11)
c (Å)	15.5389(16)	18.0123(15)
α (deg)	76.139(4)	99.254(3)
β (deg)	83.939(4)	103.778(3)
γ (deg)	79.428(4)	93.974(3)
V (Å^3)	1278.1(2)	2561.6(4)
T (K)	150(2)	150(2)
Z	2	1
D$_{calc}$ (g.cm^{-1})	1.471	1.475
μ (mm^{-1})	0.700	0.743
Total refls	24694	55584
Abs corr	multiscan	multiscan
Uniq refls (R$_{int}$)	5869(0.0500)	11719 (0.0430)
Uniq refls (I > 2σ(I))	4793	9646
R$_1$, wR$_2$	0.0583, 0.1376	0.0741, 0.2008
R$_1$, wR$_2$ (all data)	0.0732, 0.1465	0.0907, 0.2226
GOF	1.075	1.031

Notes

Supporting Information Available. Experimental procedure for the synthesis of **1b**, ^{31}P NMR spectrum of complex **5a**. Additional UV-vis-NIR figures for complexes **5a** and **6b** and DPV for complex **8.** X-ray crystallographic files in CIF format. This material is available free of charge on the ACS Publications website at DOI:

References

1 Martín, N.; Sanchez, L.; Herranz, M. A.; Illescas, B.; Guldi, D. M. *Acc. Chem. Res*. **2007**, *40*, 1015-1024.

2 Lopez-Andarias, J.; Rodriguez, M. J.; Atienza, C.; Lopez, J. L.; Mikie, T.; Casado, S.; Seki, S.; Carrascosa, J. L.; Martín, N. *J. Am. Chem. Soc*. **2015**, *137*, 893–897.

3 (a) Isla, H.; Gallego, M.; Pérez, E. M.; Viruela, R.; Ortí, E.; Martín, N. *J. Am. Chem. Soc.* **2010**, *132*, 1772–1773. (b) Bivaud, S.; Goeb, S.; Croué, V.; Dron, P. I.; Allain, M.; Salle, M. *J. Am. Chem. Soc.* **2013**, *135*, 10018–10021.

4 Moreira, L. ; Calbo, J.; Calderon, R. M. K.; Santos, J.; Illescas, B. M.; Arago, J.; Nierengarten, J.-F.; Guldi, D. M.; Orti, E.; Martín, N. *Chem. Sci.* **2015**, *6*, 4426–4432.

5 Shao, M.; Dongare, P.; Dawe, L. N.; Thompson, D. W.; Zhao, Y. *Org. Lett.* **2010**, *12*, 3050–3053.

6 Akiba, K.; Kiyofumi I.; Naoki I. *Bull. Chem. Soc. Jpn*. **1978**, *51*, 2684–2689.

7 Bryce, M. R.; Moore, A. J. *Synthetic metals* **1988**, *25*, 203–205.

8 Bryce, M. R.; Moore, A. J.; Hasan, M.; Ashwell, G. J.; Fraser, A. T.; Clegg, W.; Hursthouse, M. B.; Karaulov, A.I. *Angew. Chem. Int. Ed. Engl.* **1990**, *29*, 1450–1452.

9 Gruhn, N. E.; Macías-Ruvalcaba, N. A.; Evans, D. H. *Langmuir* **2006**, *22*, 10683–10688.

10 Perepichka, D. F., Bryce, M. R.; Perepichka, I. F.; Lyubchik, S. B.; Christensen, C. A.; Godbert, N.; Batsanov, A. S.; Levillain, E.; Mclnnes, E. J. L.; Zhao, J. P. *J. Am. Chem. Soc.* **2002***, 124*, 14227–14238.

11 (a) Pérez, E. M.; Sánchez, L.; Fernández, G.; Martin, N. *J. Am. Chem. Soc.* **2006**, 128, 7172–7173. (b) Pérez, E. M.; Capodilupo, A. L.; Fernández, G.; Sánchez, L.; Viruela, E. O.; Orti, E.; Bietti, M.; Martín, N. *Chem. Commun.* **2008**, 4567–4569. (c) Fernández, G.; Pérez, E. M.; Sánchez, L.; Martín, N. *Angew. Chem., Int. Ed.* **2008**, *47*, 1094–1097. (d) Canevet,

D.; Gallego, M.; Isla, H.; de Juan, A.; Pérez, E. M.; Martín, N. *J. Am. Chem. Soc.* **2011***, 133*, 3184−3190.

[12] Bastien, G.; Dron, P. I.; Vincent, M.; Canevet, D.; Allain, M.; Goeb, S.; Sallé, M. *Org. Lett.* **2016**, *15*, 5856−5859.

[13] Ogi, D.; Fujita, Y.; Mori, S.; Shirahata, T.; Misaki, Y. *Org. Lett.* **2016**, *15*, 5868−5871.

[14] Díaz, M. C., Illescas, B. M.; Martin, N.; Perepichka, I. F.; Bryce, M. R.; Levillain, E.; Viruela, R.; Orti, E. *Chem. Eur. J.* **2006**, *12*, 2709−2721.

[15] Martín, N.; Perez, I.; Sanchez, L.; Seoane, C. *J. Org. Chem.* **1997**, *62*, 870−877.

[16] Díaz, M. C; Illescas, B. M.; Seoane, C.; Martín, N. *J. Org. Chem.* **2004**, *69*, 4492−4499.

[17] Shao, M.; Guang, C.; Zhao, Y. *Synlett* **2008**, *3*, 371−376.

[18] Illescas, B. M.; Santos, J.; Wielopolski, Atienza, C.; Martin, N. ; Guldi, D. M. *Chem. Commun.* **2009**, 5374−5376.

[19] (a) Vacher, A.; Barrière, F.; Piekara-Sady, L.; Roisnel, T.; Lorcy, D. *Organometallics* **2011**, *30*, 3570–3578. (b) Vacher, A.; Barrière, F.; Lorcy, D. *Organometallics* **2013**, *32,* 6130–6135.

[20] (a) Colbert, M. C. B.; Lewis, J.; Long, N. J.; Raithby, P. R.; White, A. J. P.; Williams, D. J. *J. Chem. Soc., Dalton Trans.* **1997**, 99–104. (b) Jones, N. D.; Wolf, M. O.; Giaquinta, D. M. *Organometallics* **1997**, *16*, 1352–1354. (c) Lebreton, C.; Touchard, D.; Le Pichon, L.; Daridor, A.; Toupet, L.; Dixneuf, P. H. *Inorg. Chim. Acta* **1998**, *272*, 188–196.

[21] Garcia, R.; Herranz, Á.; Torres, R.; Bouit, P.-A.; Delgado, J. L.; Calbo, J.; Viruela, P. M.; Orti, E.; Martin, N. *J. Org. Chem.* **2012**, *77*, 10707−10717.

[22] Vacher, A.; Barrière, F.; Roisnel, T.; Lorcy, D. *Chem. Commun.* **2009**, 7200−7202.

[23] Younus, M.; Long, N. J.; Raithby, P. R.; Lewis, J.; Page, N. A.; White, A. J. P.; Williams, D. J.; Colbert, M. C. B.; Hodge, A. J.; Khan, M. S.; Parker, D. G. *J. Organomet. Chem.* **1999**, *578*, 198–209.

[24] Martín, N.; Sánchez, L.; Seoane, C.; Ortí, E.; Viruela, P. M.; Viruela, R. *J. Org. Chem.* **1998**, *63*, 1268–1279.

[25] Pérez, I.; Liu, S. G., Martín, N.; Echegoyen, L. *J. Org. Chem.* **2000**, *65*, 3796–3803.

[26] Christensen, C. A.; Bryce, M. R.; Batsanov, A. S.; Becher, J. *Org. Biomol. Chem.* **2003**, *1*, 511–522.

[27] Liu, S.-G.; Pérez, I.; Martín, N.; Echegoyen, L. *J. Org. Chem.* **2000,** *65,* 9092–9102.

[28] Chaudret, B.; Commenges, G.; Poilblanc, R. *J. Chem. Soc., Dalton Trans.* **1984**, 1635–1639.

[29] Shao, M.; Chen, G.; Zhao, Y. M. *Synlett* **2008**, 371–376.

[30] Sheldrick G. M., *Acta Cryst.* **2015**, *A71*, 3–8.

[31] Sheldrick G. M., *Acta Cryst.* **2015**, *C71*, 3–8.